Electronic Supplementary Material (ESI) for Lab on a Chip.

A visual portable microfluidic experimental device (PMED) with multiple electric field regulation functions

Wenshang Guo,[a] Ye Tao,[*ab] Weiyu Liu,[c] Chunlei Song,[a] Jian Zhou,[a] Hongyuan Jiang,[d] and Yukun Ren*[a]

[a.] *State Key Laboratory of Robotics and System, Harbin Institute of Technology, West Da-zhi Street 92, Harbin, Heilongjiang 150001, People's Republic of China.*

[b.] *School of Engineering and Applied Sciences and Department of Physics Harvard University, 9 Oxford Street, Cambridge, MA 02138, USA.*

[c.] *Chang'an University, Middle-Section of Nan'er Huan Road, Xi'an 710000, China.*

[d.] *School of Mechatronics Engineering, Harbin Institute of Technology, West Da-zhi Street 92, Harbin 150001, People's Republic of China.*

* *Corresponding author.*

E-mail addresses: ytao@seas.harvard.edu (Ye Tao)

rykhit@hit.edu.cn (Yukun Ren)

Supplementary Information

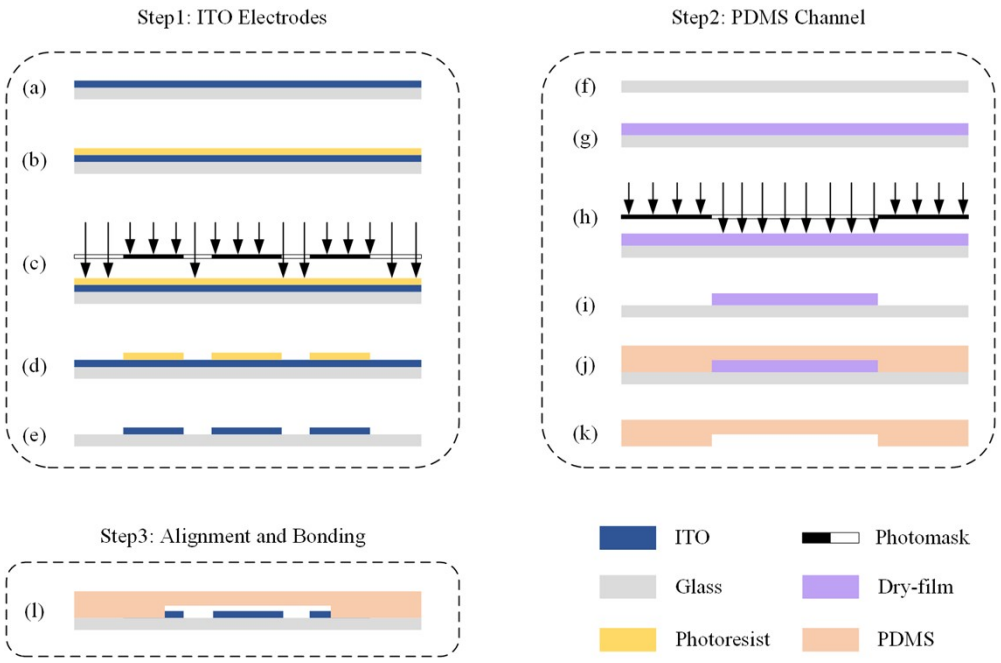

Fig. S1 The fabrication process of the microfluidic chip. (a) The ITO-coated glass slide cleaned; (b) The negative dry film laminated; (c) Ultraviolet light exposure; (d) Development; (e) ITO etching; (f) Glass cleaned; (g) Dry film stuck; (h) Ultraviolet light exposure; (i) Development; (j) Microchannel reproduced with PDMS; (k) PDMS channel stripped off; (l) Alignment and bonding.

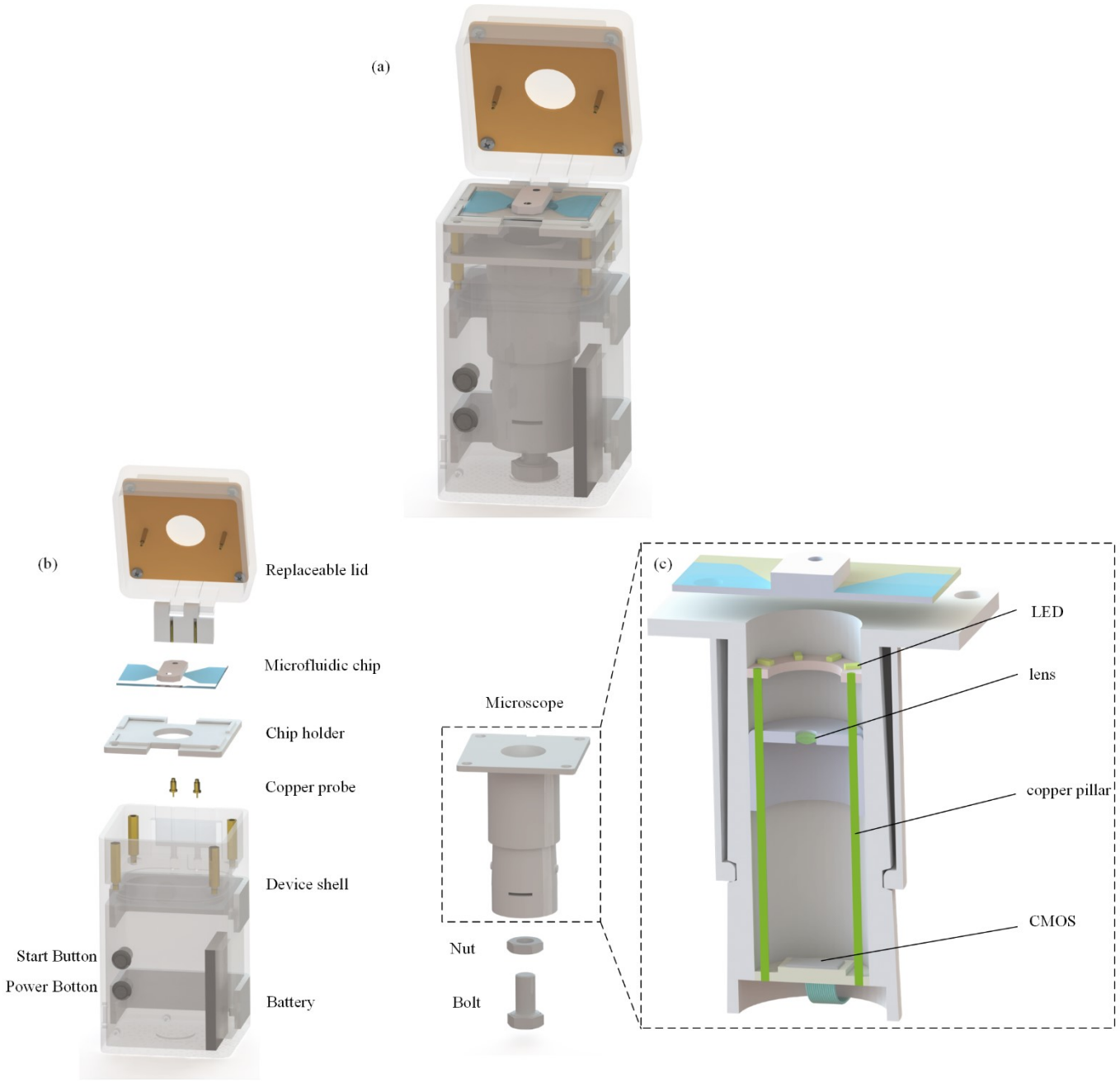

Fig. S2 Structure diagram of PMED. (a) Overall appearance structure; (b) Structural explosion diagram; (c) Sectional view of the microscope.

Note: The overall structure of PMED is shown in Fig. S2(a), and the components are shown in Fig. S2(b). PMED is composed of replaceable top cover, device shell, microscope and battery. The replaceable top cover is placed on the shell. The battery is pasted on the inner wall of the shell, and the microscope is also integrated inside the device.

A printed circuit board (PCB) capable of generating an electric field signal is installed on the replaceable top cover. There are two spring probes on the PCB. When the cover is closed, the probe contacts

the ITO electrode to realize the conduction of electrical signal (Fig. S3). To ensure the detachability of the top cover, the top cover and the device shell are connected by copper probes. After the top cover is placed on the shell, the copper pillar on the top cover will contact the copper probe on the shell, so as to transmit the power signal from the battery to the top cover.

The microscope consists of LEDs, lens, copper column, CMOS image sensor, nut and focusing bolt. The sectional view is shown in Fig. S2(c). The light source and objective lens of the microscope are on the same side of the observed object. The light from the LEDs is reflected by the surface of the measured object (microfluidic chip), irradiated on the CMOS image sensor through the lens, and then processed by the microcontroller and sent to the smartphone through WIFI. The nut is fixed under the microscope and matched with the focusing bolt. The microscope can be moved up and down by turning the focusing bolt, and the observed object can be clearly magnified by focusing.

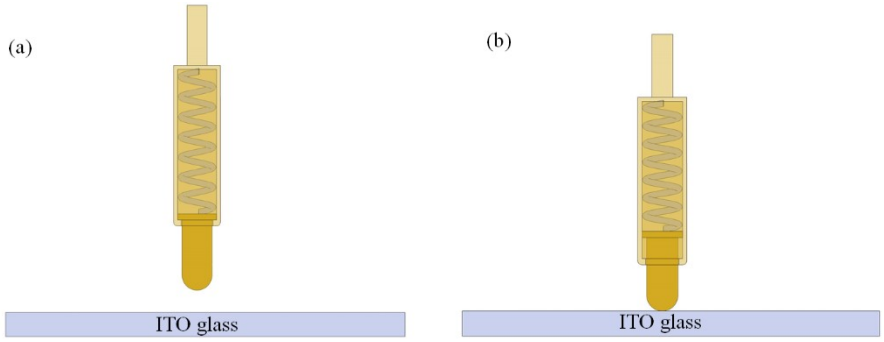

Fig. S3 (a) Probe and ITO glass; (b) The probe is in contact with the ITO glass.

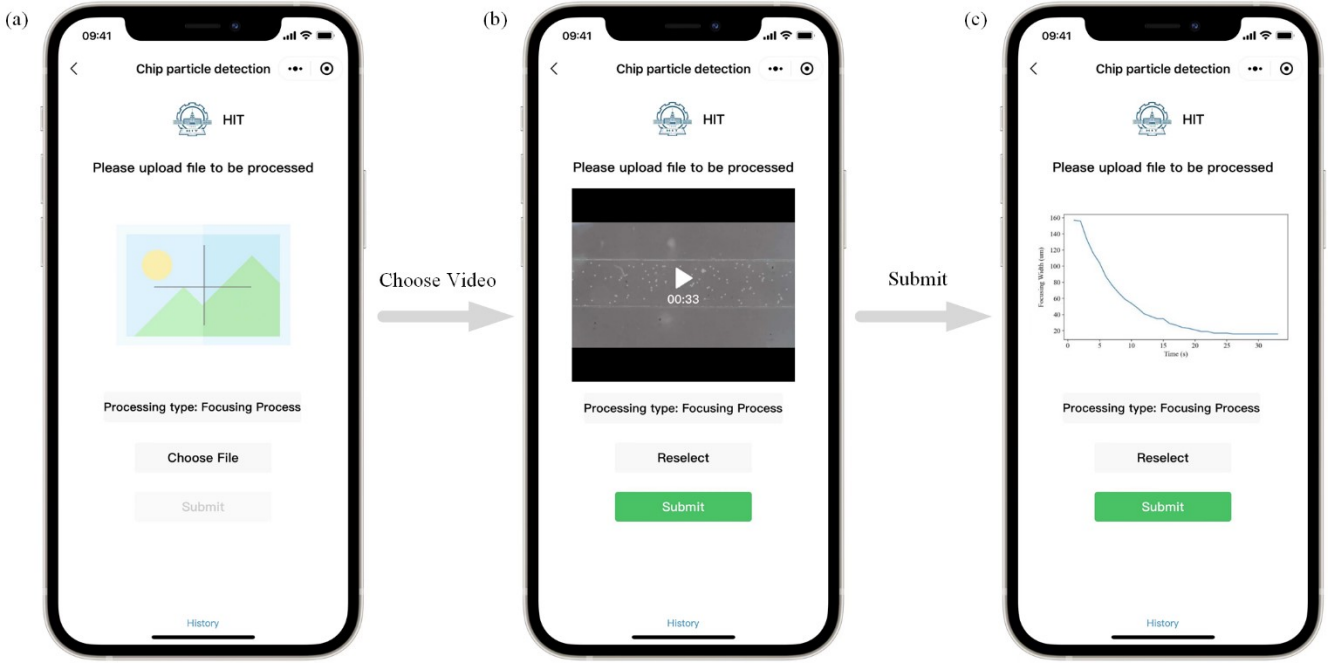

Fig. S4 App for particle focusing process analysis. (a) Initial interface; (b) Upload the video file to be analyzed; (c) Get the analysis result.

Note: The initialization interface of the APP is shown in Fig. S3(a). Click the "Choose File" button to pop up a video file selection box. Select the video file to be analyzed, and a preview of the selected video will be displayed on the APP interface (Fig. S3(b)). Then click the "Submit" button, wait for the file to be uploaded to the server and analyzed, and then the result will be displayed on the APP interface (Fig. S3(c)).

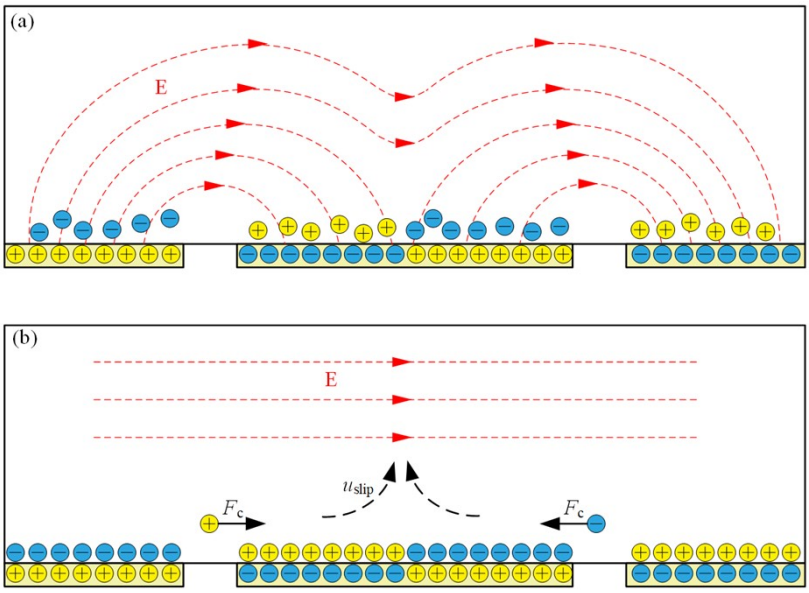

Fig. S5 Schematic illustration of the working principle of ICEO.

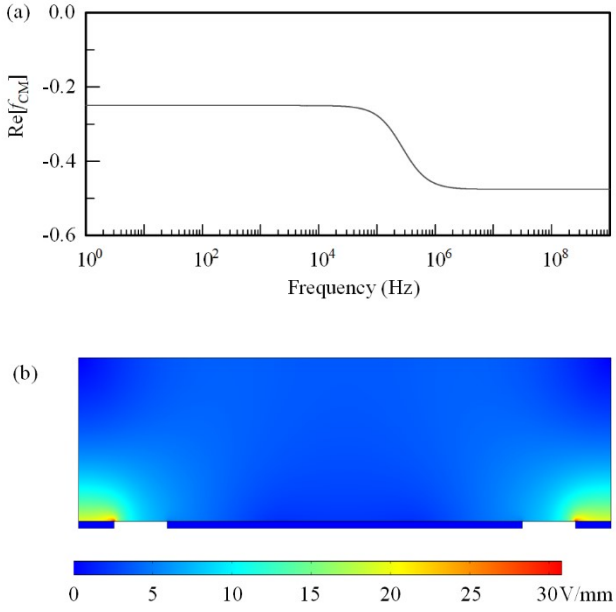

Fig. S6 (a) Frequency dependence of the real part of the CM factors in the buffer solutions; (b) Electric field distribution inside the channel.

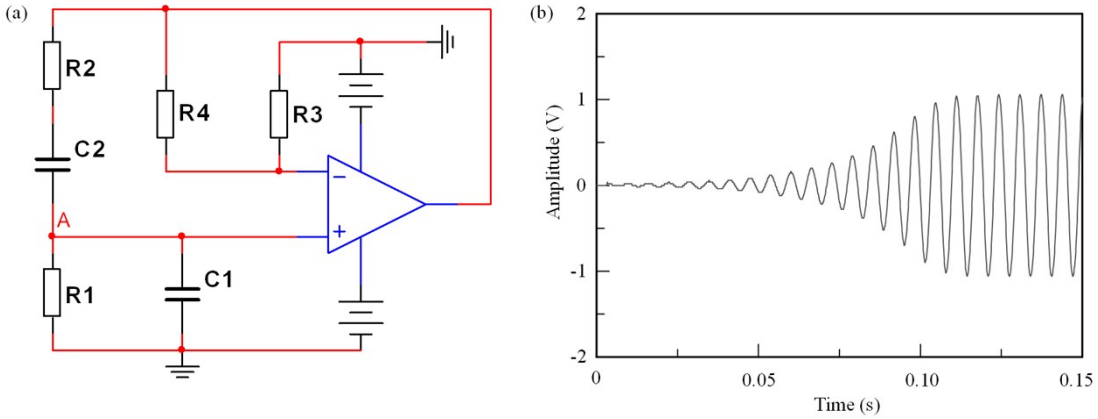

Fig. S7 (a) Basic Wien bridge oscillation circuit; (b) Circuit start-up process.

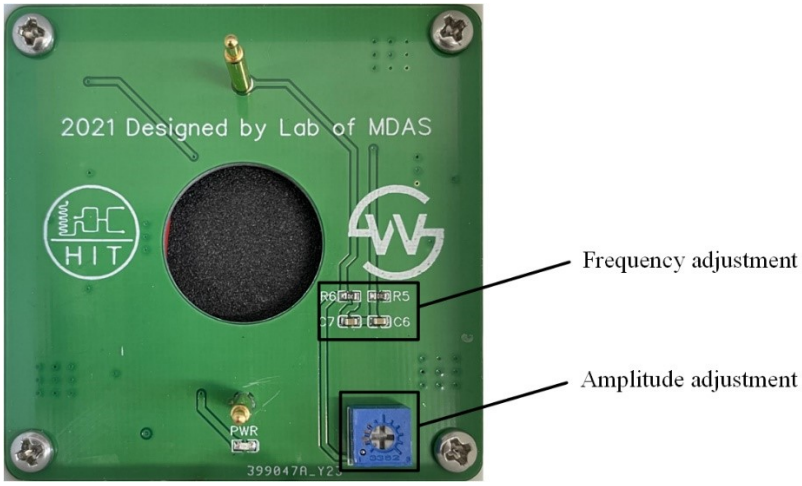

Fig. S8 Physical view of top cover.

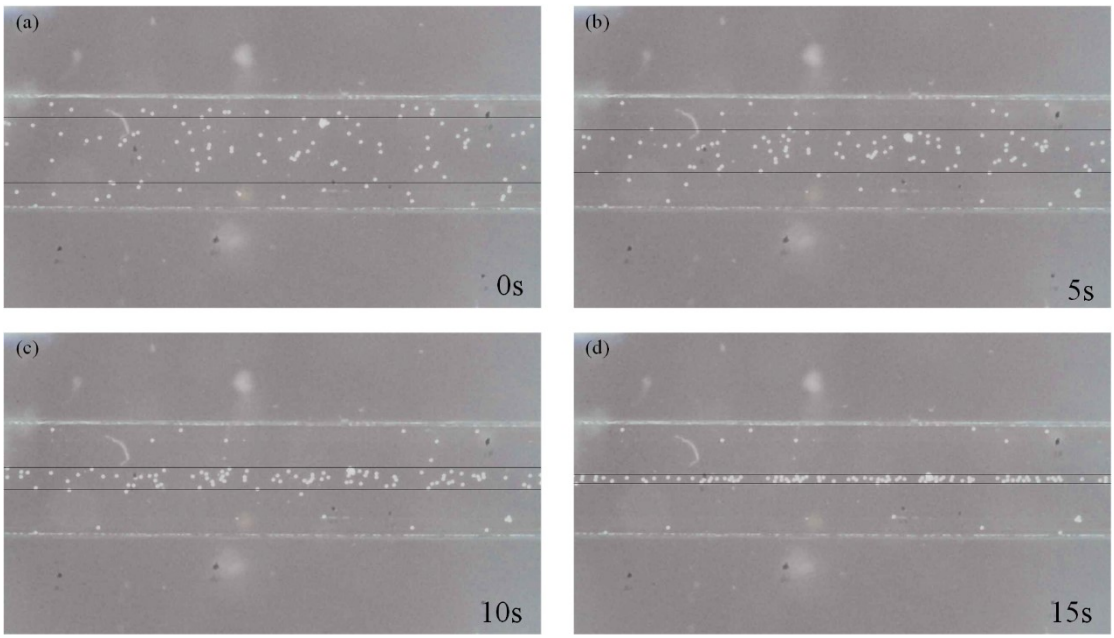

Fig. S9 Analysis of focusing process of 12 μm PS microspheres in ICEO experiment.

Steps to calculate focusing width:

(1) Draw lines on each side of the floating electrode, and move to the center of the floating electrode in units of pixels.

(2) During the moving process, calculate the sum of the grayscale values of all pixels on the line.

(3) If the grayscale value is not 0, it indicates that there are particles on the line. At this time, the two lines will stop moving, and the distance between the two lines is the focused pixel width.

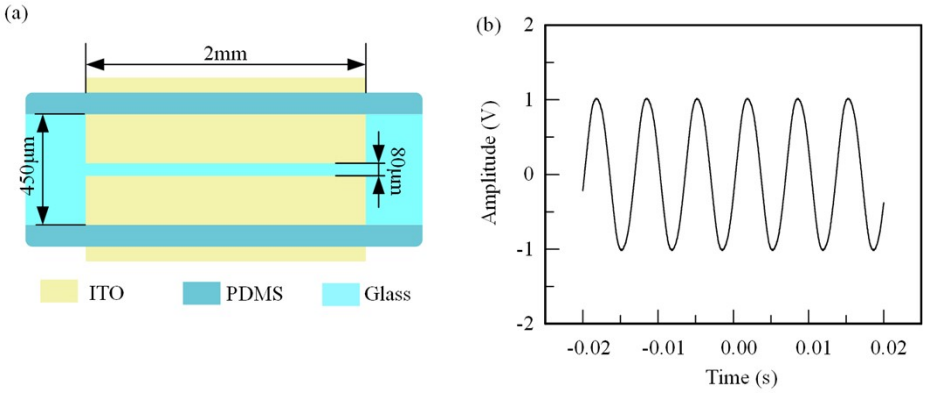

Fig. S10 (a) Structure size in ACEO experiment; (b) AC signal applied in ACEO experiment.

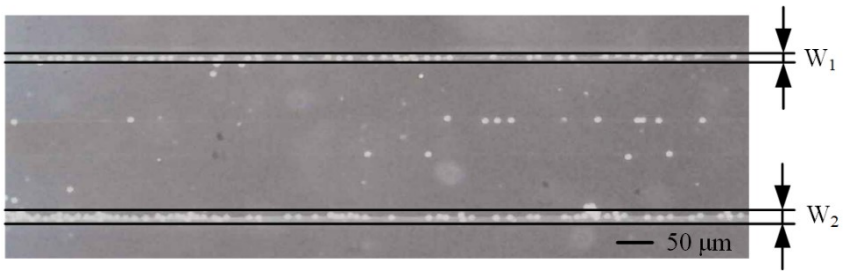

Fig. S11 Particle focusing width in ACEO experiment.

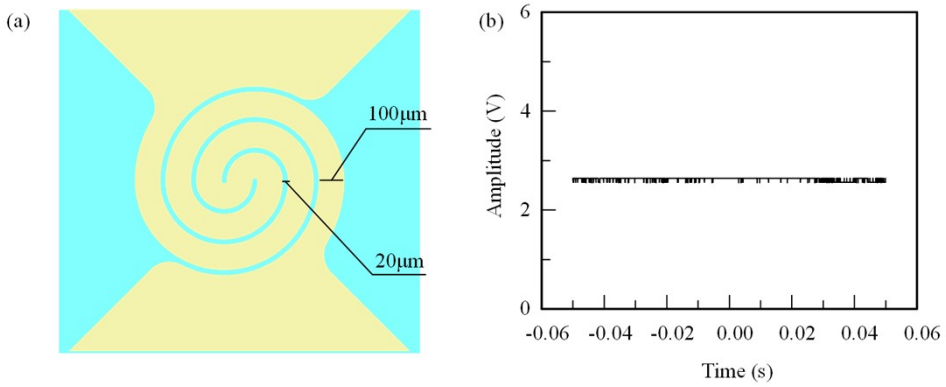

Fig. S12 (a) Structure size in thermal buoyancy convection experiment; (b) DC signal applied in thermal buoyancy convection experiment.

Note: Since the DC signal we applied is generated through the PCB, and circuit components and layout are limited by space. Under limited conditions, the generated DC signal has a certain ripple, but the overall signal fluctuation is still within an acceptable range (± 0.05 V).

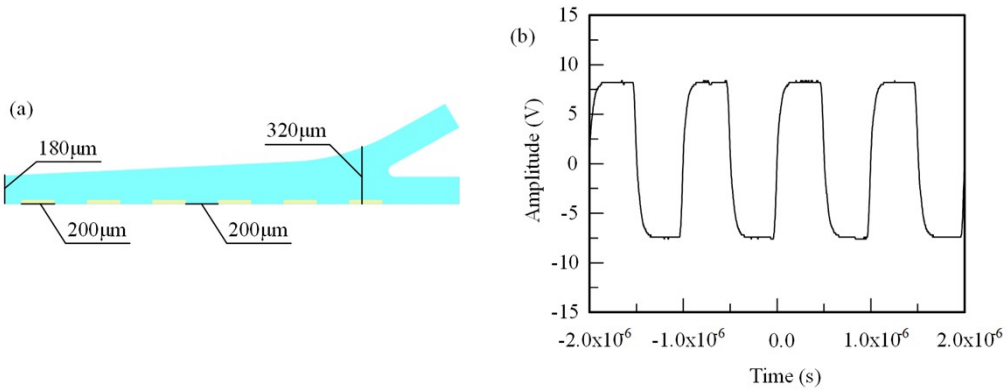

Fig. S13 (a) Structure size in DEP experiment; (b) AC signal applied in DEP experiment.

Table S1. Boundary conditions employed in the numerical simulation

Position	Condition in electric field	Condition in flow field
Electrolyte	$\nabla^2\tilde{\varphi}=0$	$-\nabla p+\nabla\cdot\left(\eta\left(\nabla u+(\nabla u)^{\mathrm{T}}\right)\right)=0,\ \nabla\cdot u=0$
The driving electrode 1	$\sigma(n\cdot\nabla\tilde{\varphi})=j\omega C_0\left(\tilde{\varphi}-A_1\right)$	$\langle u_{\mathrm{s}}\rangle=\frac{\varepsilon}{2(1+\delta)\eta}\mathrm{Re}\left(\left(\tilde{\varphi}-A_1\right)\left(\tilde{E}-\tilde{E}\cdot n\cdot n\right)^{*}\right)$
The driving electrode 2	$\sigma(n\cdot\nabla\tilde{\varphi})=j\omega C_0(\tilde{\varphi}-0)$	$\langle u_{\mathrm{s}}\rangle=\frac{\varepsilon}{2(1+\delta)\eta}\mathrm{Re}\left(\tilde{\varphi}\left(\tilde{E}-\tilde{E}\cdot n\cdot n\right)^{*}\right)$
The floating electrode	$\sigma(n\cdot\nabla\tilde{\varphi})=j\omega C_0\left(\tilde{\varphi}-\frac{A_1}{2}\right)$	$\langle u_{\mathrm{s}}\rangle=\frac{\varepsilon}{2(1+\delta)\eta}\mathrm{Re}\left(\left(\tilde{\varphi}-\frac{A_1}{2}\right)\left(\tilde{E}-\tilde{E}\cdot n\cdot n\right)^{*}\right)$
Wall	$n\cdot\nabla\tilde{\varphi}=0$	$u=0$

Where $\tilde{\varphi}=Ae^{j\theta}$ is complex phasor amplitude of electrostatic potential; p is the hydraulic pressure; u is the flow velocity; $\tilde{E}$ is the electric field phasor; ε is the electrolyte permittivity; $\delta=C_{\mathrm{d}}/C_{\mathrm{s}}$ (C_{d} is the capacitance of diffuse layer, C_{s} is the capacitance of stern layer); $\langle u_{\mathrm{s}}\rangle$ is the time-averaged ICEO slip velocity; n denotes the unit normal vector pointing into electrolyte; * indicates the complex conjugate operator.[1]

Table S2. Relationship between capacitance and oscillation frequency

C(nF)	Frequency(Hz)
220	72.343
150	106.1
100	159.15
68	234.05
47	338.63
33	482.29
22	723.43

References

1. A. González, A. Ramos, N. G. Green, A. Castellanos and H. Morgan, Physical Review E, 2000, 61, 4019-4028.